

# Research on a Buckling Detection Technique for Rectangular Concrete-filled Steel Tubular Columns based on Grating Projection

Bing Xu\*, Lang Wang, Ming-Zhi Xie

Department of Civil Engineering, Yancheng Institute of Technology, Jiangsu, China  
bateren@126.com

Received 31 March 2021; Revised 1 October 2021 ; Accepted 1 November 2021

**Abstract.** The surface buckling of concrete-filled steel tubular (CFST) columns under axial compression was observed in real time by using fringe projection, and pre-set fringes with phase information were projected onto the surface of the member. The buckling information (the size and shape of drum buckling) and its evolution were obtained by analysing the buckling images during the loading process. Nine images of key moments during the experiment were obtained by a technique of obtaining the actual measurements synchronously, and the position of the bulge on the whole side of the steel pipe was obtained by unwrapping. The shape and evolution of the drum buckling of the steel pipe developed symmetrically before point C (the ultimate bearing capacity) and evolved from 2 to 3 peaks. After passing through point C, the buckling deformation was asymmetrical. The deformation near the loading end increased gradually, and the buckling deformation increased with loading. The fastest growth stage was between points C and F, and the load displacement curve showed a rapid reduction in the load. These experimental results show that this noncontact measurement method based on fringe projection is effective in detecting the buckling of rectangular CFST column surfaces.

**Keywords:** rectangular concrete-filled steel tubular short column, local buckling, fringe, detection

## 1 Introduction

Rectangular concrete-filled steel tubular (CFST) column members are widely used in many large structural projects because of their high stiffness and high strength. The buckling of thin steel plates under an axial force easily results in bulging on the side of the steel tube, which weakens the restraint on the core concrete and therefore reduces the bearing capacity of the member [1].

Uy brain [2, 3] (1998/2000) discovered the local buckling of steel tubes in rectangular CFST members and studied the effect of local buckling on the strength of CFST column via experimentation. Bokang He, Xiaobing Yang, Tianhua Zhou [4] (2002) calculated the critical stress of rectangular CFST columns by utilizing variational principles. Shixu Mo, Renda Zhao, Xingu Zhong [5] (2005) and Xuefeng Jin, Xuewen Zhang, Jian Cai [6] (2007) calculated the expression of buckling stress under different constraints. Baokang He, Xiaobing Yang, Tianhua Zhou [7] (2005) used the finite spline method to analyse the critical stress and buckling coefficient of thin plates under different stress gradients and compared them with the Chinese code. Guohuang Yao, Yongjun Huang and Wei Tan [8] (2007) introduced the effective width [9] to revise the local buckling strength formula of rectangular CFST slabs, and the calculated bearing capacity was in good agreement with the test results. Lanhui Guo, Sumeike Zhang, Wha-Jung Kim, Gianluca Ranzi [10] (2007) studied the buckling behaviour of rectangular steel tubes and CFST members by means of experimental and finite element methods, where the specimens were designed with the width-to-thickness ratio as the design parameter. After the experiment, the buckling deformation of the members was compared. Ning Zhang, Yongjian Liu and Hui Li [11] (2015) analysed the buckling coefficient of CFST members by using the energy method. The ultimate buckling mode and ultimate buckling coefficient of the steel tube were given, and it was reported that the post-buckling strength of the steel pipe decreases with an increase in the effective width-to-thickness ratio. Lanhui Guo, Sumei Zhang [12] (2009) conducted a theoretical analysis on the bearing capacity of CFST members and found that the calculated bearing capacity without considering the buckling of plates was higher than that obtained by experiments and finite element analysis. Moreover, the buckling of rectangular steel tubes was shown to be unfavourable for the bearing capacity of the members. Xiaoxiong Zha, Ruiqiang Song, He-nan Lu [13] (2010) performed a finite element analysis to verify the relevant conclusions of previous studies. Meichun Zhu, Jianxin Liu, Qingxiang Wang, Xiufeng Feng [14] (2010) studied a rectangular steel-reinforced CFST column and reported that when the steel tube experienced

\* Corresponding Author

local buckling, the decreasing section of the load displacement curve began to stabilize, which indicates that local buckling is an important manifestation of the failure of the member and can be observed experimentally. The shape and position of the flexion evolved throughout the experiment. Lanhui Guo, Qin Rong, Sumei Zhang [15] (2011) analysed the corresponding relationship between the bulging and bearing capacity of CFST columns under axial compression and concluded that the bearing capacity of members began to decrease after the emergence of bulging. Cheng-Cheng Chen, Jen-Wen Ko, Guo-Luen Huang, Ying-Muh Chang [16] (2012) found that buckling of the lateral wall of the member occurred before the peak load, and the buckling shape changed with increasing load. Clotilda Petrus, Hanizah Abdul Hamid, Azmi Ibrahim, Gerard Parke [17] (2010) similarly discovered that the yield morphology and yield position of CFST columns with reinforced measures were concentrated at the loading position of the members, and the bulging waveforms of the members were different from those of unreinforced members. As is evident, the above research on the buckling of steel plates on the side of rectangular CFST columns is focused mainly on the influence of buckling on the bearing capacity, and only theoretical analyses can explain the relationships between the design parameters and bearing capacity. In contrast, the deformation of steel plates in structures under real stress, especially the deformation after the failure of a CFST member due to loading of the steel tubes, has scarcely been investigated, and there are no relevant studies on the appearance and evolution of drum buckling in broken steel pipes. Hence, studying the deformation and evolution of steel tube drums would be helpful for clarifying the behaviour of rectangular CFST columns [18].

Because the concrete performance during the buckling of a steel tube represents the out-of-plane deformation of the lateral steel plate (out-of-plane bulging, which will be examined and analysed in this paper), the buckling shape of the steel tube is subjected to the loading conditions and initial defects. The ratio of the stiffness of the steel tube to that of the concrete is affected by the same parameters, and thus, the position of drum buckling appears random. To better study the buckling deformation and its evolution, this paper uses the fringe projection method to measure the buckling of the steel tubes in rectangular CFST columns and demonstrates that the whole deformation field of the sidewall of the steel tube can be measured by using this method. This approach ultimately provides a fast, simple and effective method for monitoring the safety of rectangular CFST structures.

## 2. Principle of the Optical Measurement of the Buckling Characteristics of the Steel Tubes

The interaction between the steel tube and concrete in CFST members is of great engineering importance to the study of the behaviour of members after buckling [19], the performance of members in the plastic stage, and the safety of structures. Among the existing detection methods, fringe projection, a highly efficient and fast full-amplitude detection method, is an extremely effective noncontact measurement technique for detecting the shape characteristics of objects. Based on the stripes projected on the surface of an object, the geometric morphology of the component and its variation are analysed by identifying the deformation characteristics of the stripes. Li, Yu and Gao (2016) and Kang, Li, et al. (2017) showed that a sinusoidal fringe can be projected onto the plane to complete the measurement of three-dimensional objects, and the surface topography of the object can be described by calibrating the camera's internal and external parameters using three-dimensional coordinates. Such fringe projection measurements can be used as a reference for the measurement of steel tube buckling on the surface of CFST columns.

### 2.1 Fringe Projection Measurement Principle

Fringe projection can be used to measure the overall shape of an object. Using the fringes with phase information projected onto the surface of the steel tube after buckling can obviously reveal that the projection image of the stripes on the tube drum is deformed. Using a camera, the distorted grating projection image can be captured, and the related image can be parsed into a spatial digital signal whose phase and amplitude are modulated.

Fig. 1 presents a schematic diagram of the optical principle of measuring buckling waveforms by fringe projection. The coordinate system is established from the plane of the measured steel tube. The line connecting the optical centre point P of the projector to the optical centre point C of the camera is established parallel to the reference plane during the measurement. The optical axis CO of the camera and the optical axis PO of the projector intersect at point O on the object surface, and the angle between the two axes is  $\theta$ . In the measurement, the preset fringe with phase information is projected onto point H on the surface of the buckled steel tube (point H is represented as point B on the projection axis, and point H can be observed by the camera as point A); at this time, point B on the projection axis is observed as point A. Therefore, the surface distance AB can be used to acquire

the height of point H from the reference plane. By using the principles of geometric optics, the height of point H can be calculated according to the proportion (x, y):

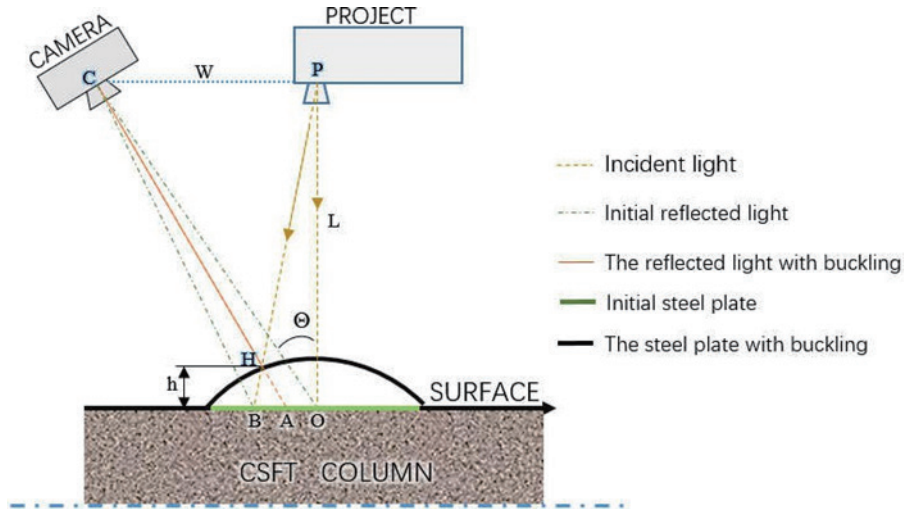


Fig. 1. Light paths of the testing for buckling

$$h_{(x,y)} = \frac{AB * L}{w + AB} \quad (1)$$

where  $w$  -- the distance between the camera centre point  $C$  and the projector centre point  $P$ ;

$L$  -- the distance from the projector to the projection axis.

By using projection equipment, a sinusoidal grid pattern parallel to the axis of the component is projected diagonally onto the surface of the component, and the image of the grid lines is photographed by the camera at a certain angle. Any pixel in the captured image has a phase value  $\phi_{(x,y)}$ . With height information corresponding to time  $t$ , the phase value of the projected image along the front grating line of the steel tube is assumed to be  $\phi_{0(x,y)}$ ; similarly, the phase value of the projected image along the grid line after buckling of the steel tube after buckling of the steel tube is  $\phi_{1(x,y)}$ . These phase values before and after the buckling of the steel tube are plotted in a graph. The phase difference of the image is:

$$\phi_{(x,y)} = \phi_{0(x,y)} - \phi_{1(x,y)} \quad (2)$$

If the frequency of the projection grating is  $f_0$ ,  $\phi(x, y)$  can be described as:

$$\Delta\phi_{(x,y)} = 2\pi \cdot f_0 \cdot AB \quad (3)$$

Formula (1) may be rewritten as:

$$h_{(x,y)} = \frac{\Delta\phi_{(x,y)} \cdot L}{2Wf_0\pi + \Delta\phi_{(x,y)}} \quad (4)$$

The height corresponding to the buckling point should be replaced by the phase shift  $\Delta\phi_{(x,y)}$ , so the main task of this method is to determine the phase shift  $\Delta\phi_{(x,y)}$  of the node.

## 2.2 Layout, Typeface, Font Sizes, and Numbering

Using point O as the origin of the coordinate system, the X axis and Y axis both pass through point O, and the Y axis is perpendicular to both the projection axis and the X axis. The intensity distribution function of the coded grid image projected onto the surface of the steel tube can be described as:

$$g_{(x,y)} = a_{(x,y)} + b_{(x,y)} \left[ 2\pi f_0 x + \phi_{(x,y)} \right] \quad (5)$$

where:  $a_{(x,y)}$  -- the distribution function of the light intensity;

$b_{(x,y)}$  -- the nonuniform reflectance function of the structure surface.

To better study the relationship between these variables, the relationship between the light intensity and grid distribution frequency in both time and space for the image projected onto the structural structure can be accurately described by using the formula above. The spatial information in formula 5 is described by the image, and the time information is represented by the frequency. The above expression is mathematically transformed into:

$$c_{(x,y)} = 0.5b_{(x,y)} \exp \left[ i \cdot \phi_{(x,y)} \right] \quad (6)$$

The expression (5) can be reworded:

$$g_{(x,y)} = a_{(x,y)} + c_{(x,y)} \exp(2\pi i f_0 x) + c_{(x,y)}^* \exp(-2\pi i f_0 x) \quad (7)$$

In formula (7),  $c_{(x,y)}$  and  $c_{(x,y)}^*$  are conjugates of each other. After applying a Fourier transform to x, formula (7) can be written as:

$$G_{(f,y)} = A_{(f,y)} + C_{(f-f_0,y)} + C_{(f+f_0,y)}^* \quad (8)$$

where  $A_{(f,y)}$  is the zero-frequency component representing the background information and  $C_{(f-f_0,y)}$  and  $C_{(f+f_0,y)}^*$  are the conjugate zero-frequency components with phase information, that is, the frequency components with the buckling and deformation information. At this point, a low-pass filter is designed to extract the fundamental frequency component  $C_{(f-f_0,y)}$  and translate it to the coordinate origin for an inverse Fourier transform. Thus,  $C_{(x,y)}$  in the time domain and the logarithm of  $C_{(x,y)}$  are obtained.

$$\log \left[ c_{(x,y)} \right] = \log \left[ 0.5 \cdot b_{(x,y)} \right] + i \cdot \phi_{(x,y)} \quad (9)$$

The imaginary part of the above formula is the principal value of the phase difference between the distorted grating lines on the object surface and the reference plane. After processing, the real phase difference and the true height of the object can be obtained.

$$h_{(x,y)} = \frac{p \cdot \phi_{(x,y)} \cdot L}{2\pi d - p \cdot \phi_{(x,y)}} \quad (10)$$

### 3. Verification of the Drum Surface Buckling Detection Technology based on Fringe Projection

To convert the above optical measurement principle into an effective measurement method to determine the bulging of a steel pipe, a BFL-722 magnetic buckle (see Fig. 2 for the size with 9.83 mm for the measured height) was used to simulate the surface bulging of the pipe before the formal test. The fringe projection method was then applied to detect buckling of the drum surface. In the measurement process, sinusoidal stripes with different phase shifts were projected onto the magnetic buckling surface, the images were analysed after collecting the relevant images, the corrected phase shift diagrams were calculated, and the out-of-plane deformation values of the structure were obtained. The images that were collected and processed during the validation test are shown in Fig. 3. To ensure optimal performance during the experiment, the projection device, camera, and positions of the three specimens were fixed. The operation steps of the experiment were as follows:

Step 1. According to the size of the experimental specimen, the period of the projection fringe was determined to be 10 pixels, and the initial phase of the fringe was adjusted. The initial phase angle can be set to  $0^\circ$ ,  $90^\circ$ ,  $180^\circ$ ,  $270^\circ$  or another special value.

Step 2. After installing the specimen on the experimental platform and adjusting the projector and camera, stripes were projected directly onto the surface of the specimen with a uniform vertical distribution. After the optical path was adjusted, both the distance between the camera and the projector and the distance between the projector and the surface of the specimen were recorded.

Step 3. The fringe image was projected onto the sample surface based on the order of the phase angles, and the fringe image of the structure surface was collected (as in Fig. 3(a)).

Step 4. The magnetic buckle was placed onto the surface of the measured specimen, the fringe image was projected onto the structure surface, and the related images were recorded (as in Fig. 3(b)).

Step 5. The collected images shown in Fig. 3 were unwrapped to obtain the phase shift information in the image (as in Fig. 3(c));

Step 6. The phase shift information from step 5 and the coordinate information were drawn together into an image (as in Fig. 3(d)), and the maximum displacement value was measured as 9.896 mm.

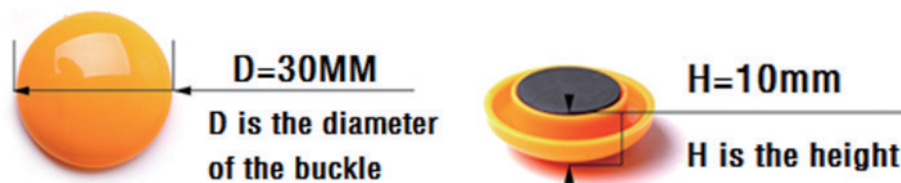


Fig. 2. Size of the magnetic buckle

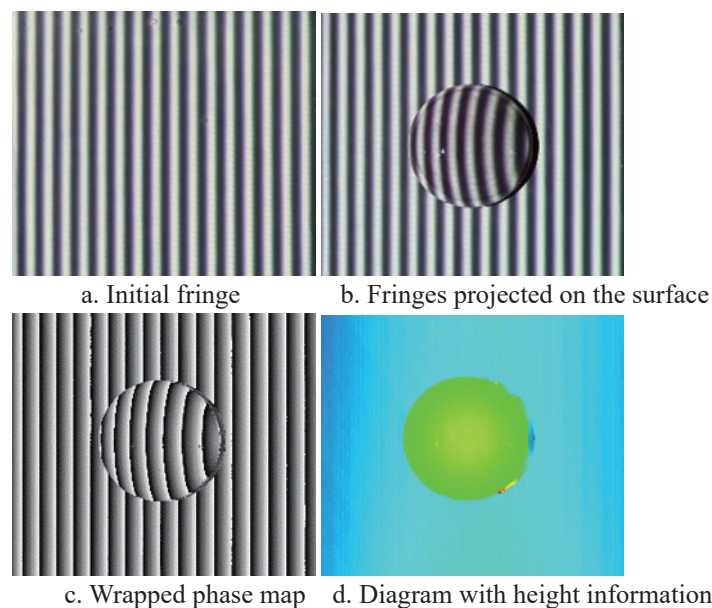


Fig. 3. Calibration chart of the measurement system

#### 4. Practical Measurement of the Buckling Behaviour of Concrete-filled Steel Tubular Short Columns

To study the buckling of the steel tube surface and the changes in the post-buckling morphology due to axial loading, a test and measurement platform was established in the laboratory (Fig. 4). Fringes with phase information were projected onto the surface of the steel tube by a projector, and relevant images were collected. In the experiment, the dimensions of the short CFST columns were 100 mm long, 100 mm wide and 300 mm high, and the steel plate was produced by the Wuhan Iron and Steel Plant with a thickness of 2 mm, manually welded, internally filled with C40 concrete, and maintained 42 days after completion of the experiment.



Fig. 4. Test machine and the fringes projected for the test

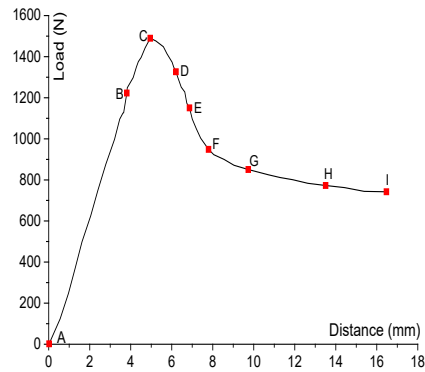
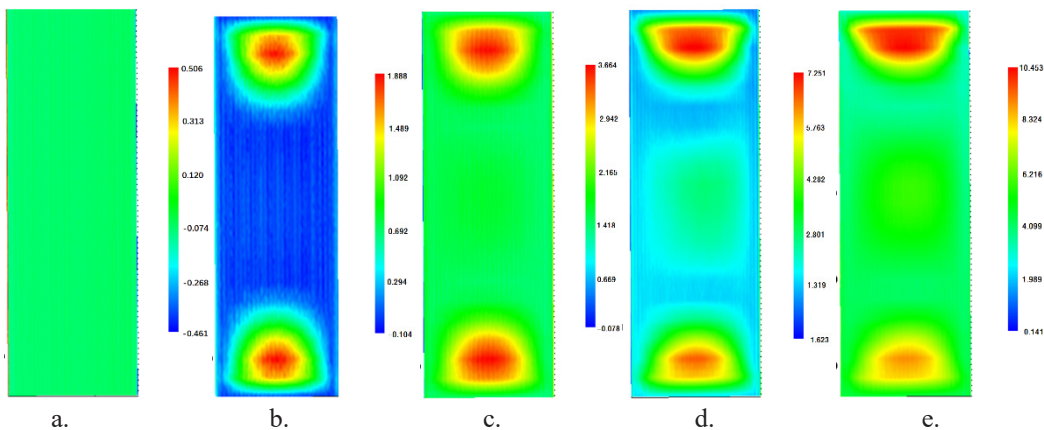


Fig. 5. Test curve

Due to the different loading times (as in Fig. 5) and the different magnitudes of deformation of the drum, the obtained fringe images vary. With increasing loading, the deformation of the buckling intensifies, the warping area of the drum rises, and the deformation range of the stripes in the image shows an increasing trend (Fig. 6). Hence, the distortion of the stripes becomes increasingly obvious. In this way, the deformation of the whole steel plate on the sidewall can be effectively detected by the measuring method, and the deformation of the steel plate can be effectively calculated. The accuracy can reach 0.01 mm, which meets the requirements of engineering studies and can be used to detect buckling during the loading process. The deformation of the lateral steel plate is out-of-plane deformation directed outward, and its shape is a sinusoidal bulge. The number of lateral bends in the buckling plates increases incrementally, and at moment B, there are 2 drum bends. During the loading process, the drum buckling of the lateral steel plate gradually becomes increasingly obvious, and the maximum deformation of the plate increases gradually.



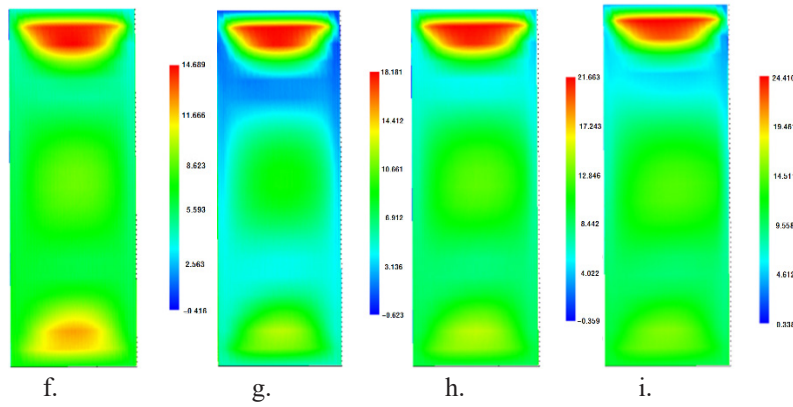
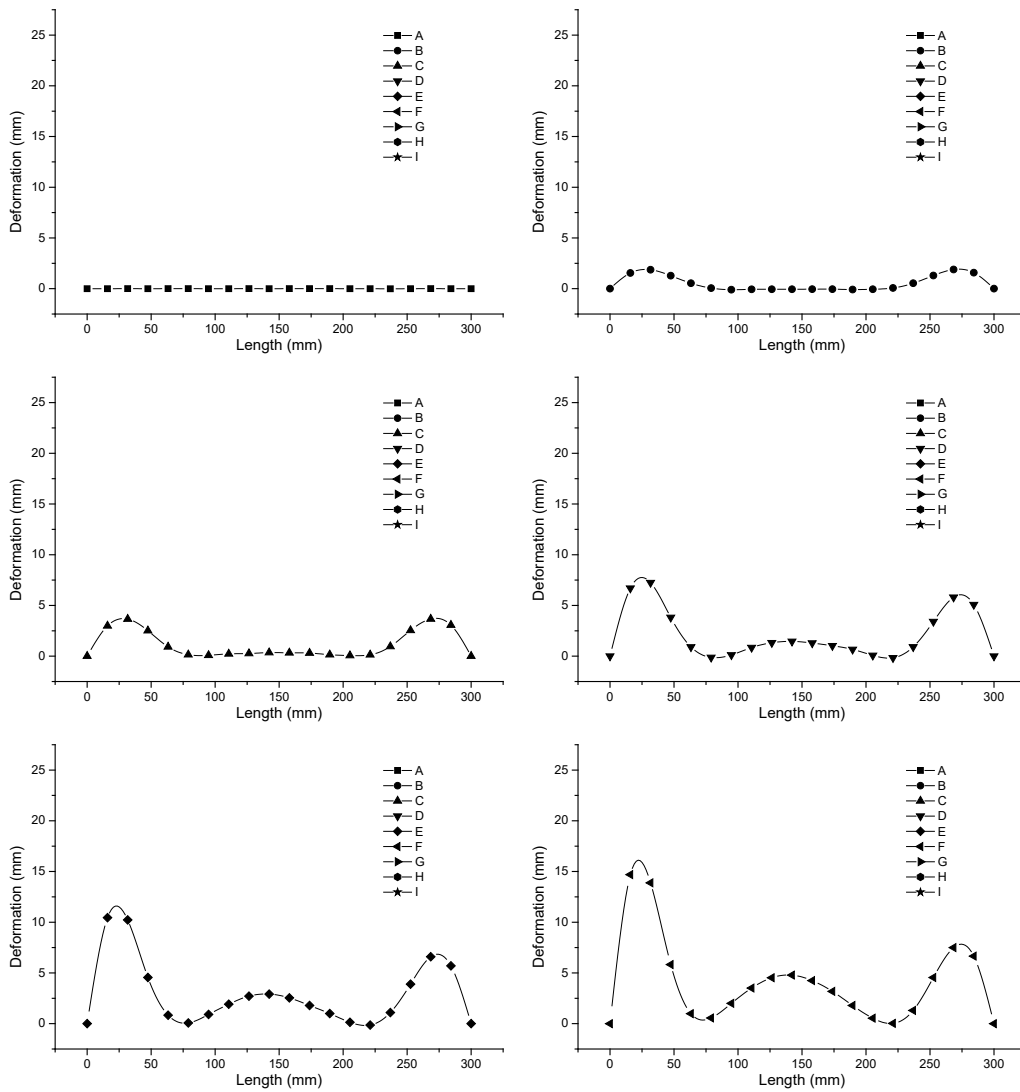


Fig. 6. Fringes on the sidewall of the steel tube at different loading times

### 5. Discussion



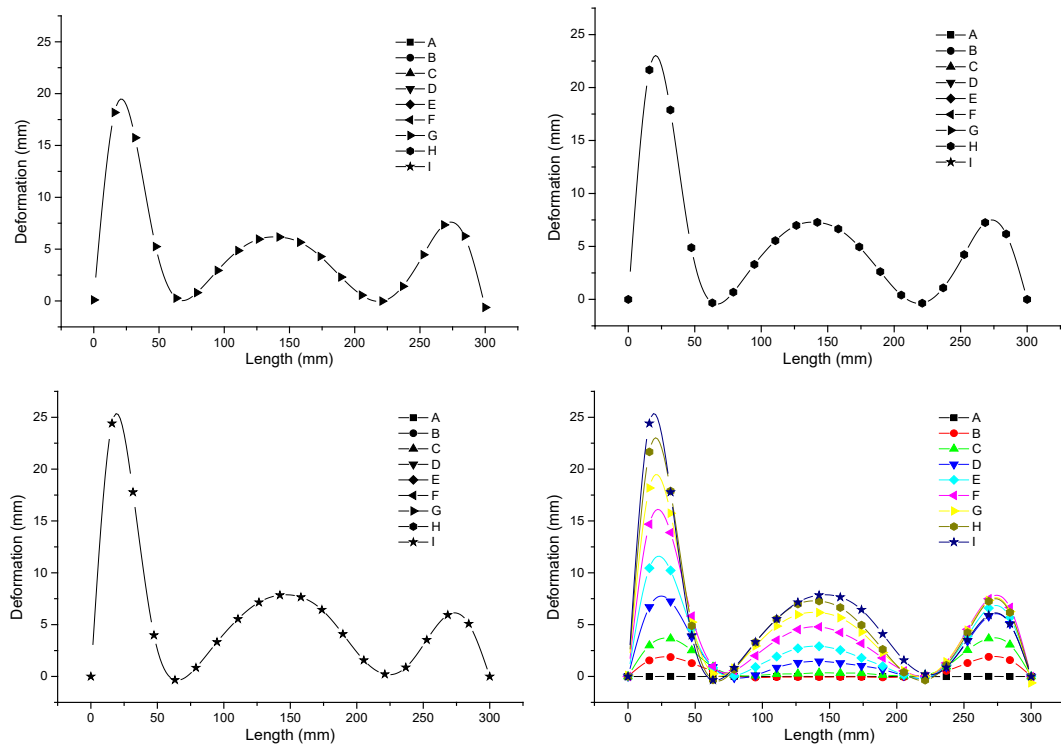


Fig. 7. Buckling deformation on the sidewall of the steel tube at different loading times

The displacement information of the steel plate along the centreline is plotted in Fig. 6, and the curves are shown in Fig. 7. Fig. 7 demonstrates that the evolution of the lateral drum deformation with axial loading can be described as follows: at the initial stage of loading (B), two symmetrical buckling locations appear on both sides of the plate under axial loading, and when loaded to moment C, the degree of deformation on both sides of the drum increases. At this moment, the centre of the sidewall begins to produce small out-of-plane deformation, 3 drums appear, and the shape of each drum is oriented along the middle of the face. At moment C, the experimental load-displacement curve enters the decreasing section, indicating that the interior concrete is damaged. According to the D-F section of the curve in Fig. 7, the deformation displacement of the outer steel pipe increases with loading, and the waveform of the buckling is asymmetric. At this moment, the amplitude and extent of the waveform near the loading end are obviously larger than those at other positions. With an increase in the experimental loading, the deformation of the waveform becomes more obvious.

The maximum displacement in the deformation curve is obtained at each moment and drawn in the curve shown in Fig. 7. According to the curve, the steel tube of the member begins to buckle at point B (the load is 82.1% of the ultimate bearing capacity), and the measured deformation is 1.96 mm (7.875% of the limit displacement). As viewed from the load-displacement curve, point B is at the elastic-plastic transition stage of the curve. Considering the deformation occurring at this moment as elastic buckling of the steel pipe, the buckling deformation at point B is recoverable after unloading. Point C is the ultimate load point. The section from point C to point F denotes the rapidly decreasing section of the loading curve; during this stage, the concrete inside the specimen is damaged, and the steel tube is plastically deformed. Hence, the bulging deformation of the lateral steel pipe includes the development of both elasticity and plastic deformation. At this stage, the maximum buckling deformation increases substantially, the slope of the displacement-deformation curve is obviously larger than that at other times. In contrast, from F to I, the load-displacement curve tends to be flat; the maximum buckling deformation of the displacement-deformation curve also increases, but the magnitude of increase (the slope) is lower than that of the curve along section C-F.

## 6. Summary and Conclusions

In this paper, a noncontact detection technique based on fringe projection is adopted to synchronously measure the lateral buckling position and shape of a rectangular CFST short column during the axial loading process, and

the technique is shown to be convenient and reliable. The flexion of the rectangular CFST member is imaged by the theoretical verification and experimental measurement of an actual component. The pattern of buckling and its evolution are detected. The following conclusions can be drawn:

1) The fringe projection method can be used to completely measure the side of a rectangular CFST column and can accurately measure the position and degree of buckling deformation, which cannot be accomplished by traditional strain measurements and is an important technical innovation.

2) The feasibility of the test method for the buckling of CFST columns is verified, and the accuracy is shown to meet the requirements of practical engineering applications.

3) According to the different deformation forms, the fringes projected onto the surface of the structure differ (Fig. 6), which shows that the fringe stripes are sensitive to the deformation of the structure and can effectively reflect the deformation characteristics of the surface. By unwrapping the fringe image, the amount of deformation can be calculated, and the true deformation value can be given. The process is convenient and reflects an efficient noncontact measurement method.

4) The image with displacements can effectively show the curvature of the drum. The differences in the images at different stages show that the fringe projection method can effectively detect the evolution of drum buckling.

5) By synchronizing the image acquisition with the loading time, the deformation of the drum can be effectively matched with the load-displacement curve of the member, and the corresponding relationship can be used. In subsequent research, the connection between steel pipe buckling and structural loading can be ascertained through a large number of tests, and the load that causes steel pipe drum buckling and its influencing parameters can be determined. This study provides an effective technical means to study the buckling and post-buckling behaviours of rectangular CFST members.

Through the research in this paper, it is shown that fringe projection is a rather effective, comprehensive and efficient noncontact method for detecting the surface buckling of rectangular CFST members and is expected to have good application prospects in engineering practice.

## Acknowledgement

This study is supported by the Foundation of Ministry of Housing and Urban-Rural Development (No. 2016-K8-009) and Natural Science Fund Project of Colleges in Jiangsu Province (No. 18KJD560006).

## References

- [1] Q.-Q. Liang, B. Uy, Nonlinear analysis of concrete-filled thin-walled steel box columns with local buckling effects, *Journal of Constructional Steel Research* 62(6)(2006) 581-591.
- [2] B. Uy, Local and post-local buckling of concrete filled steel welded box columns, *Journal of Constructional Steel Research* 47(1)(1998) 47-72.
- [3] Q.-Q. Liang, B. Uy, Theoretical study on the post-local buckling of steel plates in concrete-filled box columns, *Computers & Structures* 75(5)(2000) 479-490.
- [4] B.-K. He, X.-B. Yang, T.-H. Zhou, Theoretical analysis on local buckling behaviour of concrete filled rectangular steel tube column subjected to axis force, *Journal of Xi'an university of arcature and technology (Natural Science Edition)* (3)(2002) 210-213.
- [5] S.X. Mo, R.D. Zhao, X.G. Zhong, Local buckling research on concrete filled square steel box member, *Journal of Hunan University of Science & Technology (Natural Science Edition)* 19(3)(2004) 43-47.
- [6] X.-F. Jin, X.-W. Zhang, J. Cai, Analysis of the local buckling of the steel plates in thin-walled concrete-filled steel box columns, *Journal of Hefei University of Technology (Natural Science)* (7)(2007) 885-887.
- [7] B.-K. He, X.-B. Yang, T.-H. Zhou, Research of the local buckling behaviors for concrete-filled rectangular steel tube colimn, *Construction Structure* (3)(2002) 210-213.
- [8] G.-H. Yao, Y.-J. Huang, W. Tan, Research on the Buckling Behaviour of Concrete Filled Steel Tubes with Rectangular Sections, *Progress in Steel Building Structures* 40(5)(2007) 47-51.
- [9] C. Petrus, H. Abdul, A. Ibrahim, Experimental behaviour of concrete filled thin walled steel tubes with tab stiffeners, *Journal of Constructional Steel Research* 66(7)(2010) 915-922.
- [10] L. Guo, S. Zhang, W. Kim, G. Ranzi, Behavior of square hollow steel tubes and steel tubes filled with concrete, *Thin-Walled Structures* 45(12)(2007) 961-973.
- [11] N. Zhang, Y.-J. Liu, H. Li, Local Buckling Performance Analysis of Rectangular Concrete-filled Steel Tubular Axial Compression Column with PBL Stiffeners, *Journal of Architecture and Civil Engineering* (2)(2017) 95-102.
- [12] L.-H. Guo, S.-M. Zhang, Simplified methof of bearing capacity of concrete-filled rectangular steel tube columns consider-

- ing local buckling subjected to axial compression, *Industrial Construction* (7)(2009) 98-102.
- [13]X.-X. Zha, R.-Q. Song, H.-N. Lü, Limiting value determination of width-to-thickness ratio for thin-walled hollow concrete-filled rectangular steel tube in local buckling, *Construction Structure* (1)(2010) 19-22.
- [14]M. Zhu, J. Liu, Q. Wang, X. Feng, Experimental research on square steel tubular columns filled with steel-reinforced self-consolidating high-strength concrete under axial load, *Engineering Structures* 32(8)(2010) 2278-2286.
- [15]L.-H. Guo, Q. Rong, S.-M. Zhang, Buckling strength of square hollow section steel filled with concrete, *Journal of Harbin Institute of Technology* 43(10)(2011) 6-11.
- [16]C. Chen, J. Ko, G. Huang, Y. Chang, Local buckling and concrete confinement of concrete-filled box columns under axial load, *Journal of Constructional Steel Research* 78(2012) 8-21.
- [17]C. Petrus, H.A. Hamid, A. Ibrahim, G. Parke, Experimental behaviour of concrete filled thin walled steel tubes with tab stiffeners, *Journal of Constructional Steel Research* 66(7)(2010) 915-922.
- [18]B. Xu, F.-H. Wu, G.-Z. Xu, Mechanism Study on the Axial Compressive Performance of Short Square CFST Columns with Different Stiffeners, *Advanced in Civil Engineering* (2018) 9109371.
- [19]X. Kang, T. Li, B. Sia, A novel calibration method for arbitrary fringe projection profilometry system, *Optik - International Journal for Light and Electron Optics* 148(2017) 227-237.